ISSN 2063-5346

Investigation of microstructure, mechanical properties and fractography of Al2214/3wt%Gr_p/Xwt%B_4C_p hybrid composite

Revanna K[1,2], Suresh R[1]

[1]Department of Mechanical Engineering, VTU-CPGS, Mysuru-570029, Karnataka, India

[2]Department of Mechanical Engineering, Government Engineering College, Chamarajanagra-571313, Karnataka, India

Corresponding author: Revanna K (revannamghundi@gmail.com)

Article History: Received: 20.09.2022 **Revised:** 26.10.2022 **Accepted:** 11.11.2022

ABSTRACT

This experimental investigation reports the impact of boron carbide (B_4C_p) particles on Al2214/3%Gr_p/xB_4C_p hybrid metal matrix composites (HMMCs) at a constant weight percentage of Gr_p (3 wt.%) and x wt.% of B_4C_p particles (x = 1.5, 3, 4.5, and 6) produced by a conventional stir casting metallurgical route with bottom pouring facilities. The scanning electron microscope (SEM) combined with the energy dispersive X-ray spectroscope (EDX) shows reasonable uniform distributions of particles in the matrix phase, and a spectrum of elements present in hybrid composites with various intensities. The X-ray diffraction (XRD) analysis was performed for the phase characterization of hybrid composites. Further, the mechanical properties of Al2214 alloy and Al2214/3%Gr_p/xB_4C_p hybrid composites were studied. The experimental results of the hybrid composite revealed improved hardness and tensile properties with the addition of wt.% B_4C particles. The tensile fractured surface (SEM) micrographs revealed the root causes and mechanisms of failures in hybrid composites.

Keywords: Hybrid composites materials Gr B_4C Mechanical properties Fractography.

DOI: 10.48047/ecb/2022.11.11.26

1 Introduction

Since the various limitations of achieving combined properties like density, strength, and stiffness by conventional monolithic materials, the world has been continuously striving to explore advanced materials by refining metals and their alloys through the reinforcement of distinct materials by different metallurgical processes to exploit the best of their properties and use them in various applications. Metal matrix composites (MMCs) are unique, competent, and promising materials that have been progressively replacing conventional monolithic metals and their alloys with their improved properties through various metallurgical processes. [1,2]. Al-based MMCs are used on a large scale among the various MMCs due to their virtue of better specific strength to weight ratio, economy, and tailorable properties with different engineering demands of application [3,4]. Al-MMCs are expanding their demand to a large extent in various sectors and have been widely employed in automobiles, marine, aerospace, defense, electronics, and sports components. [5,6]. Fine particulate reinforced MMCs always have better yield strength and ductile properties than MMCs reinforced with medium and coarse particulates [7]. Most of the aluminium (Al) metal alloys were investigated with ceramic particulate reinforcement owing to their enticed improvement in their properties in combination with matrix materials [8].The hardness strength of Al MMCs was decreased by the increased addition of weight percentage of graphite particulate reinforcement, and due to the thin lubricating film formation by reinforced graphite on the composite ploughing surface, the friction is reduced, which leads to minimizing the wear on the sliding surface irrespective of the different manufacturing processes [9-12]. The MMC's wear resistance strength is improved by an accelerated wt.% of graphite particulate reinforcement in an Al alloy by sacrificing its mechanical strength. This would be balanced and improved by using graphite as a second reinforcement in a hybrid MMC with another reinforcement having supportive mechanical properties with wear resistance in a hybrid MMC [13-16]. The various reinforcement particulates are used in combination in hybrid MMCs to strengthen their mechanical properties and sliding wear resistance based on their purpose of application in different fields of engineering [17-20]. Boron carbide is one of the principal reinforcements among the different ceramic reinforcements and has some attractive properties such as decreased specific density, improved mechanical strength, excellent sliding wear resistance, low thermal expansion and chemical stability with an Al alloy [21-23]. The results of hybrid reinforcement of B_4C/Fly ash with various wt.% combinations in an A356 Al alloy MMC confirm that increasing the wt.% of B_4C improves hardness and decreases wear resistance at higher wt.% of B_4C (7.5 wt.%) of Al-B_4C/Fly ash hybrid MMC [24]. In a hybrid Al-SiC-B_4C hybrid MMCs investigation, the addition of nano particles of B_4C improved the properties such as hardness, and tensile strength of and was also distributed uniformly in the matrix phase [25]. The experimental results report the uniform reinforced particle dispersion in the matrix phase, improved hardness, density, porosity, and enhanced tensile strength with reduced ductility with successive wt.% addition of reinforcement was reported in Al6084-SiC-Gr HAMC prepared by the liquid metallurgical route [26]. The dry sliding wear strength improved substantially and a decreased friction coefficient was reported in Al6061-2SiC-xGr HMMCs fabricated via an ultrasonically assisted stir cast route at a constant 2 wt.% SiC and at various wt.% of Gr nanoparticles due to its attribution of lubrication property [27]. The results of AZ91D/B_4C/Gr HMMCs reveal the enhancement of wear resistance strength and friction coefficient with B_4C particles and the reduction of temperature in the

worn surface by Gr reinforcement due to its lubrication property at various experimental conditions [28]. HMMCs of ZA-27/Gr/aluminum experimental results reported as the graphite reinforcement is encouraged to improve the hardness, impact, and compressive strength up to 2% wt. and further addition of Gr_p leads to a reduction in the mechanical strength owing to agglomeration and crack propagation, but wear strength progressively increases with the gradual addition of graphite reinforcement in an alloy [29]

The mechanical properties of graphite (Gr) particulate-reinforced Al-based composites are strengthened by the addition of graphite (Gr) up to a limited weight percentage (3% wt.) and thereafter, the reinforcement of graphite is not favorable to improving the mechanical properties of Al-based composites. Further, with the addition of wt.% boron carbide at a constant wt.% of graphite (3% wt.), the mechanical properties such as tensile strength and hardness value of Al2214/3%Gr_p/xB_4C_p HAMCs increases owing to the high stiffness, bonding strength, and uniform distribution of B_4C with the Al matrix phase.

2 Materials and Procedure

2.1 Matrix and Reinforcements

An Al2214 alloy with an elemental composition of 3.9–5% Cu, 0.5–1.2% Mg, 0.4–1.2% Mn, 0.3% Fe, 0.5–1.2% Si, 0.25% Zn, 0.1–5% Ti, 0.1% Cr, and the rest of Al as a matrix material was used in the present work. Gr_p particulates with an average 30 μm size and 100% carbon were used as primary reinforcement at a constant 3 wt.%, and a variable percentage of B_4C_p particles with 76.46% boron and 23.54% carbon were used as secondary reinforcement with an average 60 μm size in steps of 1.5 wt.% up to 6%, as shown in Fig. 1. The table shows the designation of composite materials, which are prepared for experimental investigation with various combinations of reinforcement.

2.2 Fabrication and Experiments

The composites were repapered by a conventional stir casting (liquid metallurgical method) integrated with a bottom pouring attachment. The stir casting arrangement is equipped with different components, such as a temperature and stirrer speed controller, an electrical furnace, a graphite crucible, and a high carbon steel die. At the beginning, place the crucible in an electrical furnace for about 20–30 min at a temperature of 540 ^{0}C to eliminate the moisture content. Further, Al matrix material is weighed in accordance with the table by an electronic weighing balance, placed in a crucible, loaded into an electrical furnace to melt an alloy until the furnace temperature reaches 920 ^{0}C and held there for 30 min. to convert the matrix material to a molten state.

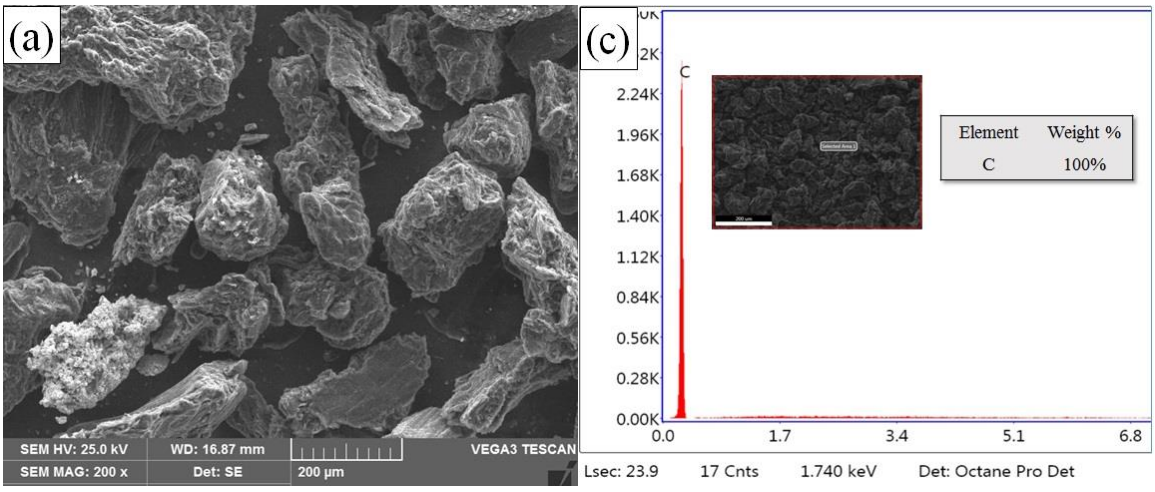

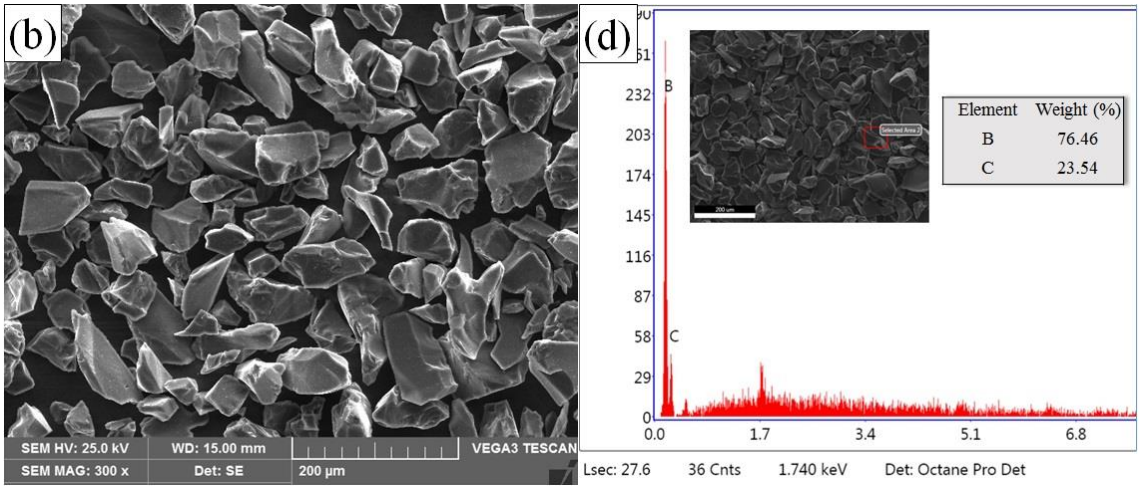

Fig 1 SEM micrographs and EDX spectrum of Gr (a) (c) and B_4Cparticles (b) (d)

The molten Al matrix was stirred to blend for about 5 min. at 200 rpm, and then about 450 ^{0}C preheated reinforcement particles of Gr_p and B_4C_p were added as per the calculation presented in the table while stirring the molten matrix. The stirring continued for 30 minutes. to ensure a proper mixture of reinforcement and matrix, and the blended molten composite was then sent to a preheated die. The die is allowed to naturally cool, and solidified composites are removed from the die when it reaches ambient temperature. The same process continues for the different combinations of matrix and reinforcements shown in the table. The samples were prepared to perform the experiments to study the microstructure, physical, and mechanical properties of composites in accordance with the ASTM standard.

Table 1. Designation of (Al2214/Gr/xB_4C) hybrid composite samples.

Al-Cu (wt.%)	Gr_p (wt.%)	B_4C_p (wt.%)	Sample code
100	0	0	A0
95.5	3	1.5	C1
94	3	3	C2
92.5	3	4.5	C3
91	3	6	C4

2.3 Experiments

The Al2214/3%Gr_p/xB_4C_p hybrid composite casting is cut into multiple pieces and prepared for microstructure studies. The samples are polished at low speed using polishing materials of 3-micron size, followed by cloth polishing to create a smooth, mirror-like surface to reveal the grain boundary at higher magnification and to improve the optical visibility of grain size microstructural and phase features. The polished samples were etched using Kellar's reagent, and after drying, the etched surface was cleaned with alcohol. The etched surface of the dried sample was investigated using a SEM combined with EDX equipment. The Al2214/3%Gr_p/xB_4C_p specimens were prepared to be examined as per ASTM standards. The rule of mixture (ROM) given by Eq. 1 is used to determine the theoretical specific density of the hybrid

composite, and the Archimedes principle is used to measure the experimental specific density given by Eq. 2. The porosity of the sample was determined by the theoretical and measured specific density values given by Eq. 3. Hardness testing of Al2214/3%Gr_p/xB_4C_p hybrid composite was carried out in accordance with ASTM standard E10-07 in a Brinell hardness tester with a ball indenter of size 10mm. The experiment is conducted at room temperature with an applied force of 10 N for a 20-second dwell period. The uniaxial tensile test was performed under the ASTM E08-8 standard with a specimen size of 9mm in diameter and 45 mm in gauge length. The specimen is stretched in a controlled condition till it breaks, and the tensile test results provide essential information such as toughness, malleability, and response with an applied axial tensile force at room temperature.

3 Result and Discussion

3.1 Microstructural studies

Fig 2 presents the SEM micrographs of specimens of as-cast Al2214 alloy and constant wt.% of Gr_p (3%) with x wt.% (3% and 6%) of B_4C Al alloy hybrid composites. The SEM micrographs of hybrid composites clearly show the existence of reinforcement Gr and B_4C particles and reasonable homogeneous dispersion in an Al matrix phase, with proof of minimal porosity in the hybrid composites produced. The interdendritic zone between Al and born carbide grains is visible in the microstructure, and there is evidence of clustering or agglomeration of reinforcement particles in the HMMCs. This was caused by the homogeneous distribution of reinforcement amid stirring and the non-variation of contact time between reinforcement particles in a liquid Al composite process. The wettability of B_4C particles with a molten Al phase was found to be good, which attributes a strong interfacial bonding between reinforcement and matrix. The porosity attributed to the casting of composites is reduced in several ways, including using an inert atmosphere (vacuum), reducing vortex motion, using baffles to generate turbulence, and maintaining appropriate speed, size, and position. At an elevated temperature, the B_4C particles were very reactive with air; hence, the reaction of the B_4C particles with trapped air in the melt reduced the pores.

The EDX is an efficient and powerful technology to determine the presence of chemical elements at different percentages in an Al2214/3%Gr_p/xB_4C_p hybrid composite specimen. The elemental mapping images of hybrid composites presented in Fig 2(d). The presence of reinforcement elements in the matrix material with alloying elements was confirmed in the EDX pattern.

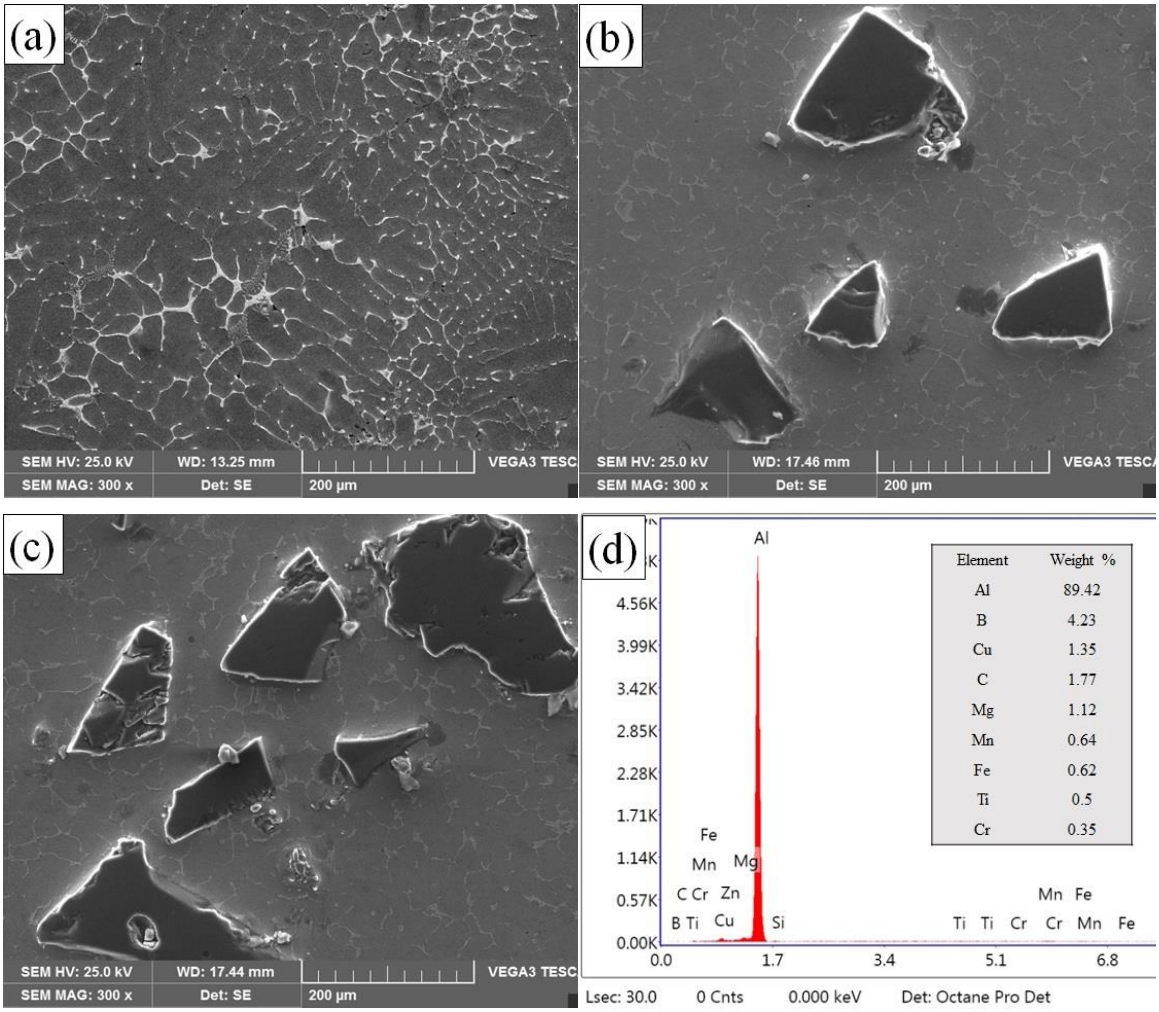

Fig 2 SEM micrographs of (a) Al2214 as-cast alloy (b) Al2214/3%Gr_p/3%B_4C_p (c) Al2214/3%Gr_p/6%B_4C_p and EDS spectrum of (d) Al2214/3%Gr_p/6%B_4C_p

The elemental analysis of the Al2214 hybrid composite with 3 wt.% of Gr_p and 6 wt.% of is presented in Fig 2(d). The EDX spectrum of composites demonstrated the presence of Gr and B_4C particles with chemical elements B and C in an Al2214/3%Gr_p/xB_4C_p hybrid composite.

The XRD analysis spectrum presented in Fig 3 conforms to the existence of reinforcement (Gr and B_4C) particles in an Al2214 matrix phase. The B_4C peaks are increasing with increased wt.% of B_4C content, while the Al peaks have decreased. It is revealed by the slight shifting of the Al peak to a lower 2θ value, which makes it evident that the reinforcements did not react with reinforcements. The reinforcement particles are thermodynamically stable at synthesised temperatures.

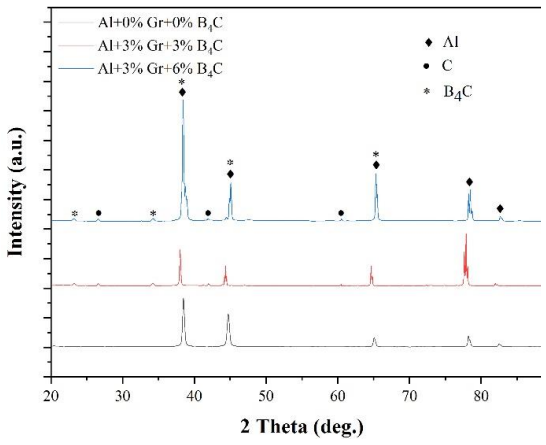

Fig 3 XRD spectrum of Al2214/Gr_p/B_4C_p hybrid composites with different wt.% of B_4C.

3.2 Specific Density

The Fig 4 shows Al2214/3%Gr_p/xB_4C_p hybrid composite densities experimentally measured (Archimedes principle) and theoretically determined (ROM) [30]. The results of densities in both methods (Archimedes principle and ROM) reveal that the addition of wt.% of reinforcements (Gr_p and B_4C_p) in an Al2214 matrix phase decreases the specific density of the Al2214/3%Gr_p/xB_4C_p hybrid composite due to the reinforcement of low densities of ceramic particles B_4C_p (2.52 g/cc) and Gr_p (2.22 g/cc).

$$\rho_{th} = \left(\frac{W_m}{\rho_m} + \frac{W_{pr}}{\rho_{pr}} + \frac{W_{sr}}{\rho_{sr}}\right)^{-1} \quad (1)$$

ρ_{th}, ρ_m, ρ_{pr} ρ_{sr} refers theoretical specific density ($g.cm^{-3}$) of hybrid composites, density of matrix and reinforcements, W_m, W_{pr} W_{sr} weight fraction of matrix and reinforcements weight fraction.

$$\rho_{exp} = \frac{m}{V} \quad (2)$$

ρ_{exp}, m V refers experimental density ($g.cm^{-3}$) of the composite, composite mass (g) and volume of water displaced (cm^3)

$$\text{Porosity}(\%) = \left(1 - \frac{\rho_{ex}}{\rho_{th}}\right) \text{x } 100 \quad (3)$$

The specific densities calculated theoretically (ROM) and experimentally (Archimedes method) are shown in Fig. 4, and the results also revealed that the theoretical specific density value of the composite is higher than the measured value, caused by the porosity attribution in the stir casting process.

3.3 Mechanical Properties

3.3.1 Hardness strength

The hardness experiment is conducted in accordance with ASTM standard E10-07 on five different places of the sample, and the average hardness (BHN) results of Al2214/3%Gr/xB_4C hybrid composite with different weight percentages (wt.%) of B_4C reinforcements are shown in Fig 5. The hardness of Al2214/3%Gr/x B_4C hybrid composites found a minimum at 3% wt. Gr and 1.5% wt. of B_4C particles, due to the presence of Gr particles in higher wt.% and their poor resistance strength to localised pressure, the further addition of wt.% (3, 4.5, and 6%) of B_4C particles in the Al2214 alloy at a constant wt.% of 3% Gr, the hardness of the Al2214/3%Gr/xB_4C hybrid composite has increased owing to the high hardness strength of secondary ceramic reinforcement (B_4C) particles.

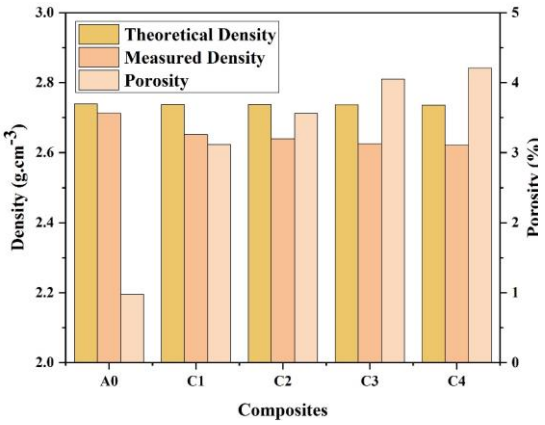

Fig 4 Specific density and porosity of Al2214/3%Gr/xB_4C hybrid composites

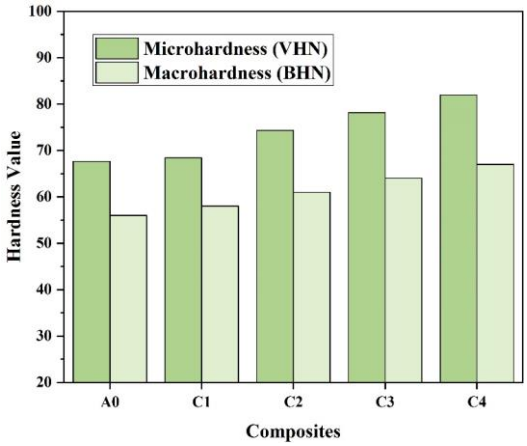

Fig 5 Hardness (BHN) of Al/3%Gr/xB_4C hybrid composites

3.3.2 Tensile properties

The tensile tests on Al2214/3%Gr/x B_4C hybrid composites were conducted at ambient atmospheric conditions. The specimens were machined and prepared as per ASTM standard E08-8. The tensile strength of MMCs is influenced by different variables such as the uniform distribution of reinforcement particles, particle size, interfacial bonding strength, etc. [31]. Fig 6 revealed the impact of the wt.% of B_4C reinforcement particles on the tensile strength of an Al2214/3%Gr/x B_4C hybrid composite. In Fig 6 the tensile strength of an Al2214/3%Gr/x B_4C hybrid composite was low at 3% wt. of Gr and 1.5 wt.% B_4C particles in the Al2214 alloy matrix phase compared to other combinations of reinforcement particles (Gr and B_4C). The low bonding strength between the Gr particles and Al matrix phase due to the slippery surface structure of Gr and the higher wettability between the interface Gr and Al phase reduces the tensile strength of Al2214/3%Gr/x B_4C hybrid composites. Further, the addition of wt.% B_4C particles at constant (3 wt.%) Gr particles in an Al2214 matrix phase increases the tensile strength of Al2214/3%Gr/x B_4C hybrid composites, the tensile properties improved essentially due to the good bonding strength of B_4C particles with the Al matrix phase.

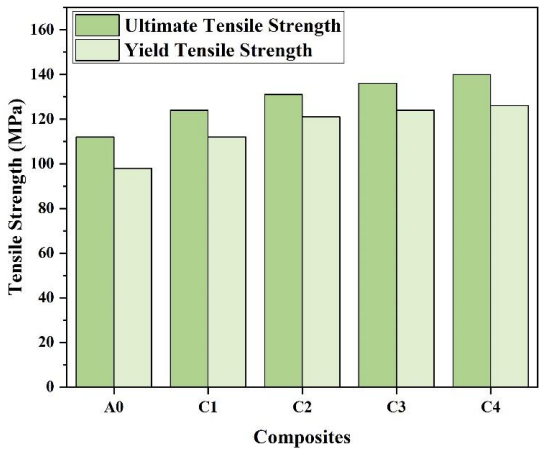

Fig 6 Tensile properties of Al/3%Gr/xB_4C hybrid composites

The wt.% of ceramic B_4C particles addition decreased the elongation percentage of in an Al2214/3%Gr/xB_4C hybrid composites. The decreased elongation primarily caused by the hard and brittle particles presence in the matrix phase. Further, the improved ductility was observed with reinforcements of 3 wt.% of Gr and 1.5 wt.% of B_4C particles in an Al2214 alloy. The Fig 7 shows variation of elongation percentage of Al2214/3%Gr/x B_4C hybrid composites with different wt.% of B_4C particles. The addition of B_4C particles reduces the ductility of the Al alloy due their brittle characteristics acts as obstacle for the deformation.

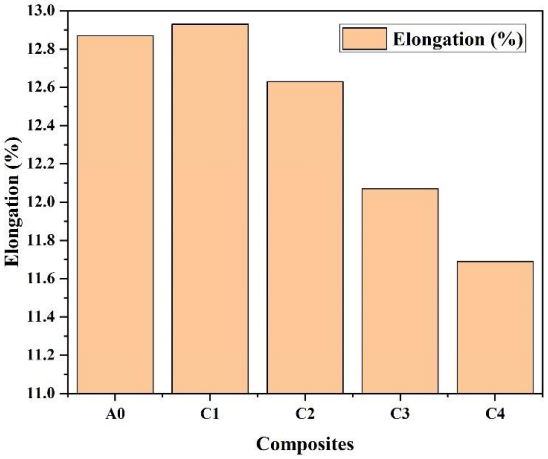

Fig 7 Elongation (%) of Al/3%Gr/xB_4C hybrid composites

3.4 Tensile Fractography

SEM micrographs of tensile fractured Al2214/3%Gr/xB_4C hybrid composite surfaces are shown in Fig 8. The tensile failure of composites revealed several-sized dimples along with an apparent neck development prior to the failure with a typical ductile fracture. The fractured surface of B_4C particle reinforced composites inherently consists of a dual-model distribution of dimples. The small dimple is connected to the ductile fracture of the matrix phase, and the large dimple is connected to particles. Further, the Al2214/3%Gr/6%B_4C specimen shows a brittle fracture in brittle mode without any appreciable neck formation with few fine

dimples, mainly owing to sudden void nucleation, expansion, and coalescence, which causes an ultimate fracture of the matrix.

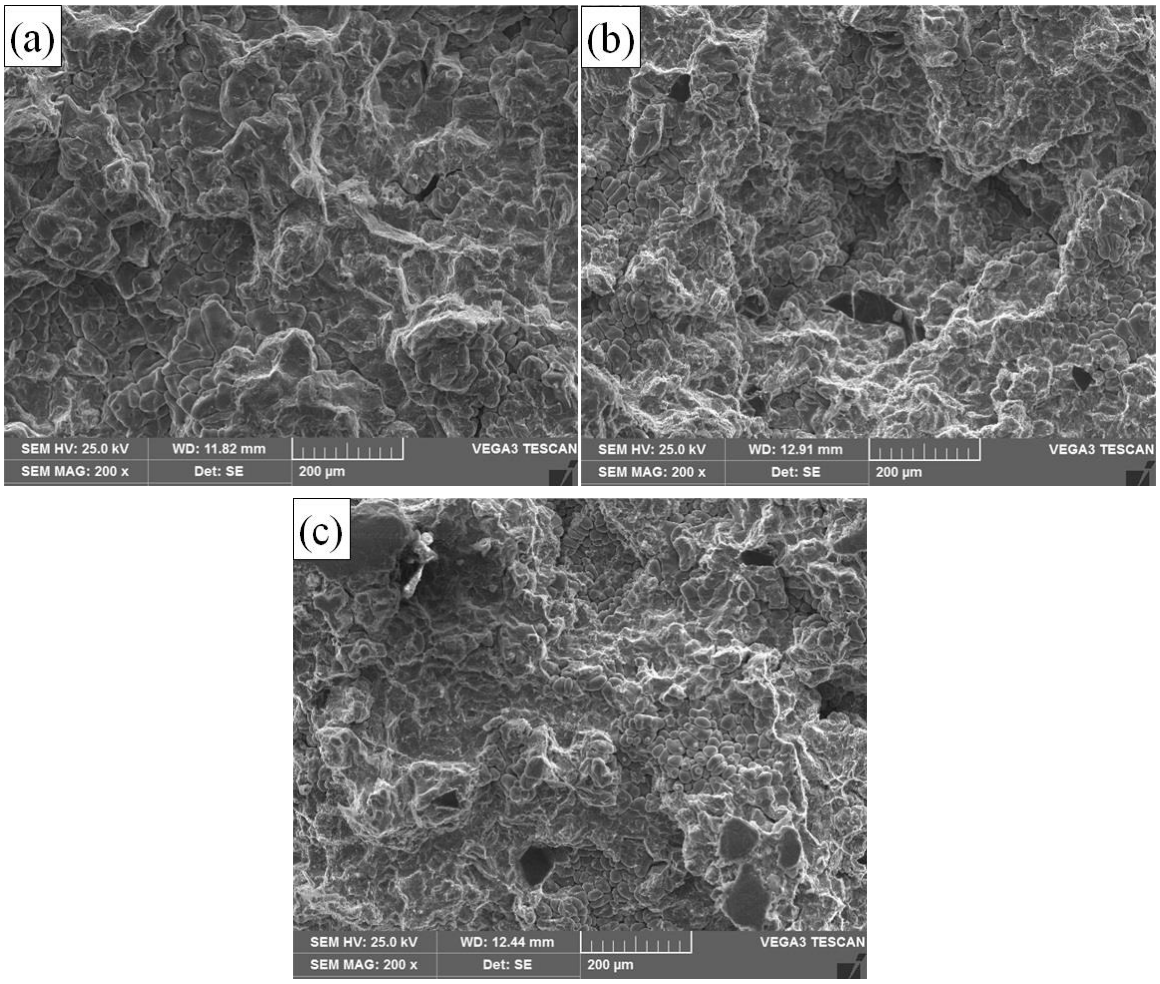

Fig 8 Tensile fractured SEM images (a) Al2214 as-cast alloy (b) Al/3%Gr_p/3%B_4C_p hybrid composite (c) Al/3%Gr_p/6%B_4C_p hybrid composite

The other possible causes to a brittle fashion of fracture of the Al2214/3%Gr/xB_4C composites may be existence of poor intermetallic phases. The presence of detrimental intermetallic phase initiate the various fracture failure mechanism of composites owing to reinforcement particles cracking, nucleation of void partially deboning interface between particles and matrix, void growth and coalescence in the matrix. The modes of fracture occur mainly on processing, distribution and morphology of hybrid composites.

4 Conclusion

The following conclusions were drawn from the present studies of hybrid Al2214/3%Gr/xB_4C composites successfully produced via a liquid metallurgical stir casting route.

(1) The SEM micrograph revealed the uniform dispersion of reinforcement particles in the matrix phase, and the elements present at different intensities with phases in the composites are confirmed by the EDX spectrum and X-RD patterns.
(2) The experimental results revealed that the specific density of hybrid

composites decreased with increased wt.% Gr and B_4C particles owing to the lower density of ceramic particles,

(3) The hardness value of HMMCs increased with the addition of B_4C particles at constant wt.% (3% wt.) of graphite.

(4) Tensile properties of Al2214/3%Gr_p/3%B_4C_p hybrid composites increased with the addition of B_4C particles in a hybrid composite

(5) The fractography studies show the mode of tensile failure; with the addition of B_4C particles, brittle fractures were observed due to the decreased ductility of hybrid composites.

References

1. Rohatgi, P. K. (1993). Metal matrix composites. Defence science journal, 43(4), 323
2. Froes, F. H. (1994). Advanced metals for aerospace and automotive use. Materials Science and Engineering: A, 184(2), 119-133.
3. Christy, T. V., Murugan, N., & Kumar, S. (2010). A comparative study on the microstructures and mechanical properties of Al 6061 alloy and the MMC Al 6061/TiB2/12p. Journal of Minerals & Materials Characterization & Engineering, 9(1), 57-65.
4. Rohatgi, P. K., & Schultz, B. (2007). Lightweight metal matrix nanocomposites–stretching the boundaries of metals. Material Matters, 2(4), 16-21.
5. Macke, A., Schultz, B. F., & Rohatgi, P. (2012). Metal matrix composites. Adv. Mater. Processes, 170(3), 19-23.
6. Miracle, D. B. (2005). Metal matrix composites–from science to technological significance. Composites science and technology, 65(15-16), 2526-2540.
7. Velasco, F., Da Costa, C. E., & Torralba, J. M. (2002). Mechanical properties and wear behaviour of PM aluminium composite reinforced with (Fe3Al) particles. Powder metallurgy, 45(3), 247-250.
8. Yigezu, B. S., Mahapatra, M. M., & Jha, P. K. (2013). Influence of reinforcement type on microstructure, hardness, and tensile properties of an aluminum alloy metal matrix composite.
9. Hassan, A. M., Tashtoush, G. M., & Al-Khalil, J. A. (2007). Effect of graphite and/or silicon carbide particles addition on the hardness and surface roughness of Al-4 wt% Mg alloy. Journal of composite materials, 41(4), 453-465.
10. Shivaprakash, Y. M., Ramu, H. C., Kumar, R., & Kumar, D. (2018, February). Experimental studies on Al (5.7% Zn) alloy based hybrid mmc. In IOP Conference Series: Materials Science and Engineering (Vol. 310, No. 1, p. 012004). IOP Publishing.
11. Akhlaghi, F., & Zare-Bidaki, A. (2009). Influence of graphite content on the dry sliding and oil impregnated sliding wear behavior of Al 2024–graphite composites produced by in situ powder metallurgy method. Wear, 266(1-2), 37-45.
12. Omrani, E., Moghadam, A. D., Menezes, P. L., & Rohatgi, P. K. (2016). Influences of graphite reinforcement on the tribological properties of self-lubricating aluminum matrix composites for green tribology, sustainability, and energy efficiency—a review. The International Journal of Advanced Manufacturing Technology, 83(1), 325-346.
13. Baradeswaran, A., Vettivel, S. C., Perumal, A. E., Selvakumar, N., & Issac, R. F. (2014). Experimental investigation on mechanical behaviour, modelling and optimization of wear parameters of B4C and graphite reinforced aluminium hybrid

composites. Materials & Design, 63, 620-632.
14. Baradeswaran, A., & Perumal, A. E. (2014). Study on mechanical and wear properties of Al 7075/Al2O3/graphite hybrid composites. Composites Part B: Engineering, 56, 464-471.
15. Aherwar, A., Patnaik, A., & Pruncu, C. I. (2020). Effect of B4C and waste porcelain ceramic particulate reinforcements on mechanical and tribological characteristics of high strength AA7075 based hybrid composite. Journal of Materials Research and Technology, 9(5), 9882-9894.
16. Suresha, S., & Sridhara, B. K. (2010). Effect of silicon carbide particulates on wear resistance of graphitic aluminium matrix composites. Materials & Design, 31(9), 4470-4477.
17. Mittal, P., Paswan, M. K., Sadasivuni, K. K., & Gupta, P. (2020). Structural, wear and thermal behaviour of Cu–Al2O3–graphite hybrid metal matrix composites. Proceedings of the Institution of Mechanical Engineers, Part L: Journal of Materials: Design and Applications, 234(8), 1154-1164.
18. Kumar, G. V., Venkatesh Chowdary, G., Surya Vamsi, M., Jayarami Reddy, K., Nagaral, M., & Naresh, K. (2021). Effects of addition of Titanium Diboride and Graphite Particulate Reinforcements on physical, mechanical and tribological properties of Al6061 Alloy based Hybrid Metal Matrix Composites. Advances in Materials and Processing Technologies, 1-18.
19. Ahamad, N., Mohammad, A., Sadasivuni, K. K., & Gupta, P. (2020). Phase, microstructure and tensile strength of Al–Al2O3–C hybrid metal matrix composites. Proceedings of the Institution of Mechanical Engineers, Part C: Journal of Mechanical Engineering Science, 234(13), 2681-2693.
20. Gangwar, S., Payak, V., Pathak, V. K., Jamwal, A., & Gupta, P. (2020). Characterization of mechanical and tribological properties of graphite and alumina reinforced zinc alloy (ZA-27) hybrid metal matrix composites. Journal of Composite Materials, 54(30), 4889-4901.
21. Kalaiselvan, K., Murugan, N., & Parameswaran, S. (2011). Production and characterization of AA6061–B4C stir cast composite. Materials & Design, 32(7), 4004-4009.
22. Kumar, M. S., Pruncu, C., Harikrishnan, P., Begum, S. R., & Vasumathi, M. (2020). Experimental investigation of in-homogeneity in particle distribution during the processing of metal matrix composites. Silicon.
23. Rajesh, G. L., Auradi, V., & Kori, S. A. (2016). Mechanical behaviour and dry sliding wear properties of ceramic boron carbide particulate reinforced Al6061 matrix composites. Transactions of the Indian Ceramic Society, 75(2), 112-119.
24. Kumar, M. S., Vasumathi, M., Begum, S. R., Luminita, S. M., Vlase, S., & Pruncu, C. I. (2021). Influence of B4C and industrial waste fly ash reinforcement particles on the micro structural characteristics and mechanical behavior of aluminium (Al–Mg–Si-T6) hybrid metal matrix composite. journal of materials research and technology, 15, 1201-1216.
25. Poovazhagan, L., Kalaichelvan, K., Rajadurai, A., & Senthilvelan, V. (2013). Characterization of hybrid silicon carbide and boron carbide nanoparticles-reinforced aluminum alloy composites. Procedia Engineering, 64, 681-689.
26. Sharma, P., Dabra, V., Sharma, S., Khanduja, D., Sharma, N., Sharma, R., & Saini, K. (2019). Microstructure and properties of AA6082/(SiC+ graphite)

hybrid composites. Refractories and Industrial Ceramics, 59(5), 471-477.
27. Prasad Reddy, A., Vamsi Krishna, P., & Rao, R. N. (2019). Tribological Behaviour of Al6061–2SiC-xGr Hybrid Metal Matrix Nanocomposites Fabricated through Ultrasonically Assisted Stir Casting Technique. Silicon, 11(6), 2853–2871.
28. Aatthisugan, I., Rose, A. R., & Jebadurai, D. S. (2017). Mechanical and wear behaviour of AZ91D magnesium matrix hybrid composite reinforced with boron carbide and graphite. Journal of magnesium and alloys, 5(1), 20-25.
29. Gangwar, S., Payak, V., Pathak, V. K., Jamwal, A., & Gupta, P. (2020). Characterization of mechanical and tribological properties of graphite and alumina reinforced zinc alloy (ZA-27) hybrid metal matrix composites. Journal of Composite Materials, 54(30), 4889-4901.
30. Prasad, D. S., Shoba, C., & Ramanaiah, N. (2014). Investigations on mechanical properties of aluminum hybrid composites. Journal of materials research and technology, 3(1), 79-85.
31. Tahamtan, S., Emamy, M., & Halvaee, A. (2014). Effects of reinforcing particle size and interface bonding strength on tensile properties and fracture behavior of Al-A206/alumina micro/nanocomposites. Journal of Composite Materials, 48(27), 3331-3346.